Investigation of thermal cut-off energy for accurate analysis of High Temperature Engineering Test Reactor

Satoshi Takeda[1]
Osaka University
Osaka, Suita, Yamadaoka 2-1, Japan
e-mail: takeda@see.eng.osaka-u.ac.jp

Takanori Kitada
Osaka University
Osaka, Suita, Yamadaoka 2-1, Japan
e-mail: kitada@see.eng.osaka-u.ac.jp

Akio Yamamoto
Nagoya University
Furo-cho, Chikusa-ku, Nagoya, Japan
e-mail: a-yamamoto@energy.nagoya-u.ac.jp

Kazuya Yamaji
Mitsubishi Heavy Industries, Ltd.
Wadasaki-cho 1-chome, Hyogo-ku, Kobe, Japan
e-mail: kazuya.yamaji.pc@nu.mhi.com

Hiroki Koike
Mitsubishi Heavy Industries, Ltd.
Wadasaki-cho 1-chome, Hyogo-ku, Kobe, Japan
e-mail: hiroki.koike.kw@nu.mhi.com

Koji Asano
Mitsubishi Heavy Industries, Ltd.
Wadasaki-cho 1-chome, Hyogo-ku, Kobe, Japan
e-mail: koji.asano.8q@nu.mhi.com

ABSTRACT

This study investigates the appropriate thermal cut-off energy for neutron transport calculations in the High Temperature Engineering Test Reactor (HTTR). Using the Monte Carlo calculation code MVP3.0, the impact of changing thermal cut-off energy on the multiplication factor was evaluated for the single fuel element geometry of HTTR, focusing on variations in fuel and moderator temperatures at the beginning of life (BOL)

[1] Corresponding author.

and end of life (EOL). In the default model of MVP3.0, resonance scattering is approximated by the free-monatomic-gas model with constant cross section. Therefore, the impact of using the exact model for resonance scattering was additionally examined. In the free-monatomic-gas model, a thermal cut-off energy of 30 eV is at least required to maintain the multiplication factor error within approximately ±50 pcm for both BOL and EOL. In addition, the results show that the impact of using the exact model instead of the free-monatomic-gas model on the multiplication factor is more than 200 pcm in the 30 to 40 eV range where U-238 has large resonance at 37 eV, and the impact becomes less than 50 pcm above 40 eV. These results indicate that a thermal cut-off energy of at least 30 eV is necessary without considering the effects of the exact model, and the energy range up to the 37 eV resonance needs to be considered in the case of applying the exact model to obtain the saturated results on multiplication factor for HTTR.

1 Introduction

The thermal motion of target nuclei and the effects of bonds within molecules and lattices need to be considered in neutron scattering cross-sections for accurate neutron transport calculations. In general, the thermal cut-off energy, which is the maximum neutron incident energy for considering thermal motion, is specified in the reactor analysis.

The asymptotic slowing-down scattering model is generally employed for scatterings with energies higher than the thermal cut-off energy [1]. In this model, it is assumed that the target nuclide does not move during the scattering. Therefore, this model does not consider neutron up-scattering. The use of the asymptotic slowing-down scattering model can be justified at higher neutron energies since the energy gain from up-scattering can be neglected. At energies below the thermal cut-off energy, a model that considers up-scattering due to the thermal vibrations of the target nuclide is

employed. In the energy range, the scattering cross-section model typically uses S(α,β) data instead of the free-monatomic-gas model if S(α,β) data are available.

The High-Temperature Gas-cooled Reactor (HTGR) is a highly safe reactor expected to be used as a versatile heat source for applications such as hydrogen production. In Japan, the High-Temperature Engineering Test Reactor (HTTR) [7,8], a 30 MW prismatic-type HTGR with coated particle fuel, was constructed to establish this technology, and analyses have been performed to ensure its performance and safety. However, in HTGR analyses, including those for the HTTR, the thermal cut-off energy has often been set below 10 eV [2-4].

In our previous study [5], calculations were performed using the Monte Carlo calculation code MVP3.0 [6] to examine appropriate thermal cut-off energy using the single fuel geometry of the HTTR. As the default model of MVP3.0, the asymptotic slowing-down scattering model is used for energies above the thermal cut-off energy, and the free-monatomic-gas model with constant cross section is used for energies below the thermal cut-off energy. The free-monatomic-gas model with constant cross section assumes a constant resonance scattering cross section at 0 K when calculating the energy and angle distributions of scattered neutrons. However, it has been confirmed that this model underestimates the up-scattering probability for resonance scattering with U-238 compared to the exact model [9]. Therefore, in addition to discussions using the free-monatomic-gas model with a constant cross section, it is expected to consider the impact of using the exact model.

Therefore, the present study discusses the thermal cut-off energy for accurate analysis of HTTR considering the difference in multiplication factor between the free-monatomic-gas model with constant cross section and the exact model. Similar to our previous research, calculations were performed using MVP3.0 with the single fuel geometry of the HTTR. Section 2 presents the calculation conditions, Section 3 shows appropriate the thermal cut-off energy estimated by the free-monatomic-gas model with constant cross section, Section 4 discusses the difference in multiplication factor between the free-monatomic-gas model with constant cross section and the exact model, and Section 5 concludes this study.

2 Calculation condition

MVP3.0 was used for the evaluation of the impact of changing the thermal cut-off for the analysis of a single fuel element geometry of the HTTR. The effects were evaluated by changing a parameter ETHMAX, corresponding to the thermal cut-off energy. In these calculations, the impact of changing ETHMAX was investigated by either increasing the fuel temperature or the moderator temperature independently. To account for the upper temperature limit of 1600°C during transient events in the HTTR [10], fuel temperatures were analyzed in the range of 300 to 1900 K. Considering the maximum reactor outlet coolant temperature of 950°C [7], graphite temperatures were analyzed in the range of 300 to 1300 K.

When increasing the fuel temperature, all temperatures within the fuel compact (including the fuel kernel, coating, and matrix materials) were changed. In the case of

increasing the moderator temperature, the carbon outside the fuel compact (including burnable poison pellets) was changed. The graphite sleeve's temperature and the helium temperature were fixed at 1000K in these calculations. These evaluations were performed for both the Beginning Of Life (BOL) and the End Of Life (EOL).

The uranium enrichment at the BOL was set at 6.7 wt%. Burn-up calculations were performed using the burn-up calculation code MVP-BURN [11] to determine the fuel composition at the EOL. For these calculations, the linear power density was determined assuming a reactor core power of 30 MWth, an effective fuel length of 2.9 m, and 30 fuel elements. Since this study does not aim to evaluate the impact on power distribution, the average fuel composition is used for all fuel compacts in the calculation of EOL condition. The calculation conditions and geometry are shown in Table 1 and Fig. 1, respectively. As shown in Fig. 1, the fuel element consists of 33 fuel compacts and 2 burnable poison pellets. The boundary condition outside the system is reflective. The statistical geometry model in MVP3.0 was used for the coated fuel particles in the fuel compacts.

Section 3 discusses ETHMAX necessary to perform accurate calculations using the default models of MVP. However, even in the energy region below ETHMAX, the default models do not strictly account for both the thermal motion of target nuclei and the energy dependence of resonance cross sections. Therefore, Section 4 examines the impact when the exact model is used for resonance scattering.

In the calculations presented in Section 3, for the discussion of appropriate thermal cut-off energy, the free-monatomic-gas model with a constant cross-section was applied below ETHMAX, while the asymptotic model was employed for energies above

ETHMAX. These settings reflect the default model configurations in MVP. For these calculations, we used a library based on JENDL-5 [12], which is the latest JENDL library.

For the analyses in Section 4, focusing on the impact of the exact model, the free-monatomic-gas model with a constant cross-section was applied below ETHMAX, while the exact model was utilized above it. To utilize the exact model, a special cross-section library is required for MVP calculation since the standard MVP cross-section libraries do not contain elastic scattering data at 0 K. Special cross-section libraries for U-235, U-238, Pu-238, Pu-239, Pu-240, Pu-241, Pu-242, and Am-241 were created based on JENDL-4 [13] for implementing the exact model in MVP [9]. Therefore, the calculations using the exact model were performed with special cross-section libraries based on JENDL-4 for these heavy nuclides and with standard MVP libraries based on JENDL-4 for other nuclides.

While Sections 3 and 4 respectively use JENDL-4 and JENDL-5, using different evaluated nuclear data libraries is considered acceptable because it doesn't significantly affect the discussion of the energy range in which thermal motion should be treated rigorously.

The number of neutron histories per batch is 10,000, the number of effective batches is 4,000, and the number of discarded batches is 100. The standard deviation of the multiplication factor is from 7 to 14 pcm in these calculations.

3 Results with free-monatomic-gas model with constant cross-section

Figure 2 shows the multiplication factors at the BOL under a fuel temperature of 1900K and a moderator temperature of 300K, with varying thermal cut-off energies.

Figure 3 presents the corresponding multiplication factors at EOL under the same temperature conditions. Figures 2 and 3 indicate that when the thermal cut-off energy is 4 or 20 eV, the multiplication factor shifts significantly towards the negative side compared to cases where the thermal cut-off energy is 30 eV or higher. With a thermal cut-off energy of 10 eV, the multiplication factor approaches the values of cases with 30 eV or higher, rather than those observed at 4 or 20 eV. This is due to the underestimation of capture rates near the 6.7 eV resonance of U-238 when the thermal cut-off energy is 10 eV, as indicated in our previous study [5]. From these figures, it can be seen that the thermal cut-off energy needs to be 30 eV or higher to maintain the multiplication factor error within approximately ±50 pcm under high fuel temperature conditions for both BOL and EOL.

Tables 2 and 3 present the comparisons of multiplication factors with varying fuel temperatures. These tables also show the differences in multiplication factors compared to the case where the thermal cut-off energy is 30 eV. The differences in multiplication factors tend to increase as fuel temperature rises because higher fuel temperatures lead to more neutron up-scattering. For both BOL and EOL, when the fuel temperature increases, it is observed that the case with a thermal cut-off energy of 10 eV is closer to the case with a thermal cut-off energy of 30 eV compared with the case with 20 eV. When the fuel temperature is 1900 K, the difference for a thermal cut-off energy of 4 eV is more negative than -200 pcm, around -50 pcm for 10 eV, and more negative than -150 pcm for 20 eV.

Similarly, Tables 4 and 5 show comparisons for varying moderator temperatures. With an increase in moderator temperature, if the thermal cut-off energy is set above 10 eV, the impact on the multiplication factor remains within approximately ±50 pcm for both BOL and EOL. No significant difference in the effect of thermal cut-off energy is observed between BOL and EOL.

Based on the above results, to maintain the multiplication factor error within ±50 pcm for both BOL and EOL under high fuel or moderator temperature conditions, it is necessary to set the thermal cut-off energy to 30 eV or higher. However, since resonance scattering is approximately treated by the free-monatomic-gas model with a constant cross-section in these results, the impact of treating resonance scattering rigorously will be discussed in the next section.

4 Results with exact model

This section discusses the impact on the multiplication factor when resonance scattering is rigorously considered using the exact model in MVP3.0. In MVP 3.0, the exact model applies to resonance reactions at energies above ETHMAX. Therefore, the influence of the exact model can be approximately discussed by changing ETHMAX. However, it is important to note that changing ETHMAX not only reflects the effects of applying the exact model but also includes the impact of changing the thermal cut-off energy on neutron scatterings other than resonance scattering of U-235, U-238, Pu-238, Pu-239, Pu-240, Pu-241, Pu-242, and Am-241. Section 3 shows that, if resonance scattering is approximately considered by the free-monatomic-gas model, variations in

the multiplication factor are within approximately ±50 pcm when ETHMAX is 30 eV or higher. Therefore, this section discusses the impact of varying ETHMAX above 30 eV, where the impact of changing ETHMAX is primarily due to the difference in resonance scattering models.

Table 6 shows the difference in multiplication factor with varying ETHMAX using the exact model at BOL when the fuel temperature is 1900 K. Table 6 shows a notable difference (-237 pcm) when ETHMAX changes from 30 eV to 40 eV. Figure 4 illustrates the total cross-sections of carbon, O-16, U-235, and U-238, showing a prominent resonance of U-238 around 37 eV within the energy range of 30 to 40 eV. The figure was generated using JANIS [14] with cross-section data at 300 K from JENDL-4. This indicates that applying the exact model has a non-negligible impact due to large resonance scattering around 37 eV of U-238, which is much larger than those of other nuclides. Table 6 also shows the impact of changing ETHMAX is less than 50 pcm when ETHMAX is higher than 40 eV. It indicates that the energy range up to the 37 eV resonance needs to be considered in the case of applying the exact model to maintain the multiplication factor error less than approximately ±50 pcm.

Figure 5 shows the impact of changing ETHMAX on the multiplication factor with varying fuel temperature using the exact model at BOL. As shown in Fig. 5, when ETHMAX changes from 30 eV to 40 eV, the impact on the multiplication factor increases as the fuel temperature rises, and the magnitude of difference exceeds approximately 100 pcm at 1000 K. The same tendency is also shown at EOL (Fig. 6). Since the fuel temperatures

exceed 1000 K in typical prismatic HTGRs, this result indicates that the exact model should be applied up to the resonance scattering around 37 eV for high-accuracy analysis.

This study highlights the necessity of applying the exact model to resonances up to 37 eV for accurate calculations. However, since the exact model is applied only to neutron energies above ETHMAX in the calculations, the effects of applying the exact model to relatively lower-energy resonances, such as the 6.7 eV and 21 eV resonances of U-238, have not been evaluated. Addressing this limitation remains a subject for future investigation.

5 Conclusion

In this study, we aimed to identify an appropriate thermal cut-off energy for accurate analysis of HTTR. We evaluated the impact of varying thermal cut-off energy under conditions of various fuel and moderator temperatures at both BOL and EOL using MVP3.0.

First, in the analysis using the free-monatomic-gas model with constant cross-section, it was found that a higher thermal cut-off energy is required when the fuel temperature is high, compared to cases with high moderator temperature. When the fuel temperature is 1900 K, a thermal cut-off energy of at least 30 eV is required to maintain the multiplication factor error within ±50 pcm. At BOL with a fuel temperature of 1900 K, when the thermal cut-off energy is set to 4 eV, the multiplication factor is underestimated by more than 200 pcm compared to that with a thermal cut-off energy of 30 eV, and by

about 150 pcm with a cut-off energy of 20 eV. There is no significant difference in the effect of the thermal cut-off energy between BOL and EOL.

Additionally, the calculation with exact model was performed to rigorously account for resonance scattering. At BOL with a fuel temperature of 1900 K, the impact of applying the exact model on the multiplication factor is more than 200 pcm for energy from 30 eV to 40 eV and less than 50 pcm above 40 eV.

The findings indicate that a thermal cut-off energy of at least 30 eV is needed if the exact model is not considered, and the energy range up to the 37 eV resonance scattering needs to be considered in the case of applying the exact model to obtain the saturated results for HTTR analysis.

References

[1] Ouisloumen, M., Sanchez, R., 1991, "A Model for Neutron Scattering Off Heavy Isotopes That Accounts for Thermal Agitation Effects," Nuclear Science and Engineering, 107(3), pp. 189-200. https://doi.org/10.13182/NSE89-186.

[2] Fukaya, Y., et al., 2020, "Self-shielding Effect of Double Heterogeneity for Plutonium Burner HTGR Design," Annals of Nuclear Energy, 138, p. 107182. https://doi.org/10.1016/j.anucene.2019.107182.

[3] Takamatsu, K., et al., 2014, "Experiments and Validation Analyses of HTTR on Loss of Forced Cooling Under 30% Reactor Power," Journal of Nuclear Science and Technology, 51(11-12), pp. 1427-1443. https://doi.org/10.1080/00223131.2014.967324.

[4] Takamatsu, K., et al., 2014, "Spontaneous Stabilization of HTGRs Without Reactor Scram and Core Cooling—Safety Demonstration Tests Using the HTTR: Loss of Reactivity Control and Core Cooling," Nuclear Engineering and Design, 271, pp. 379-387. https://doi.org/10.1016/j.nucengdes.2013.12.005.

[5] Takeda, S., et al., 2024, " Thermal cut-off energy for accurate analysis of prismatic high-temperature gas-cooled reactor," Proceedings of the 31th International Conference on Nuclear Engineering (ICONE31), Prague, Czech Republic, August 4-8, 2024, ICONE31-130801.

[6] Nagaya, Y., et al., 2017, "MVP/GMVP Version 3: General Purpose Monte Carlo Codes for Neutron and Photon Transport Calculations Based on Continuous Energy and Multigroup Methods," JAEA-Data/Code 2016-018.

[7] Shiozawa, S., et al., 2004, "Overview of HTTR Design Features," Nuclear Engineering and Design, 233(1-3), pp. 11-21. https://doi.org/10.1016/j.nucengdes.2004.07.016.

[8] Saito, S., et al., 1994, "Design of High Temperature Engineering Test Reactor (HTTR)," JAERI-1332.

[9] Mori, T., Nagaya, Y., 2009, "Comparison of Resonance Elastic Scattering Models Newly Implemented in MVP Continuous-Energy Monte Carlo Code," Journal of Nuclear Science and Technology, 46(8), pp. 793-798. https://doi.org/10.1080/18811248.2007.9711587.

[10] Maruyama, S., et al., 1988, "Core thermal and hydraulic design of High Temperature Engineering Test Reactor (HTTR)," Japan Atomic Energy Research Institute, JAERI-M-88-255.

[11] Okumura, K., et al., 2000, "Validation of a Continuous-Energy Monte Carlo Burn-up Code MVP-BURN and Its Application to Analysis of Post Irradiation Experiment," Journal of Nuclear Science and Technology, 37(2), pp. 128-138. https://doi.org/10.1080/18811248.2000.9714876.

[12] Iwamoto, O., et al., 2023, "Japanese evaluated nuclear data library version 5: JENDL-5," Journal of Nuclear Science and Technology, 60(1), pp. 1–60. https://doi.org/10.1080/00223131.2022.2141903.

[13] Shibata, K., et al., 2011, "JENDL-4.0: A New Library for Nuclear Science and Engineering," Journal of Nuclear Science and Technology, 48(1), pp. 1–30. https://doi.org/10.1080/18811248.2011.9711675.

[14] Soppera, N., Bossant, M., and Dupont, E., 2014, "JANIS 4: An Improved Version of the NEA Java-based Nuclear Data Information System," Nuclear Data Sheets, 120, pp. 294-296. https://doi.org/10.1016/j.nds.2014.07.071.

295 **Figure Captions List**
296

Fig. 1 Single fuel element geometry

Fig. 2 Multiplication factors with varying thermal cut-off energy at BOL when fuel temperature is 1900K and moderator temperature is 300K

Fig. 3 Multiplication factors with varying thermal cut-off energy at EOL when fuel temperature is 1900K and moderator temperature is 300K

Fig. 4 Total cross-sections of carbon, O-16, U-235, and U-238

Fig. 5 Change in multiplication factor with varying ETHMAX using the exact mode at BOL

Fig. 6 Change in multiplication factor with varying ETHMAX using the exact mode at EOL

297

298

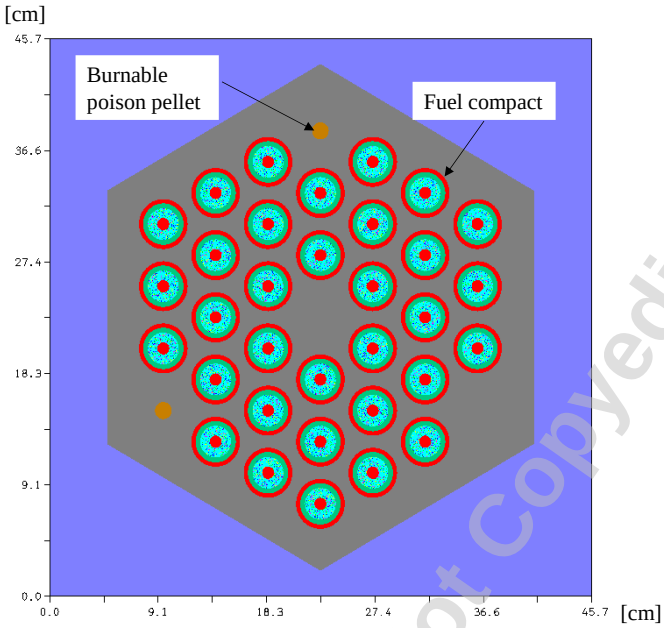

299
300 Fig. 1 Single fuel element geometry
301
302

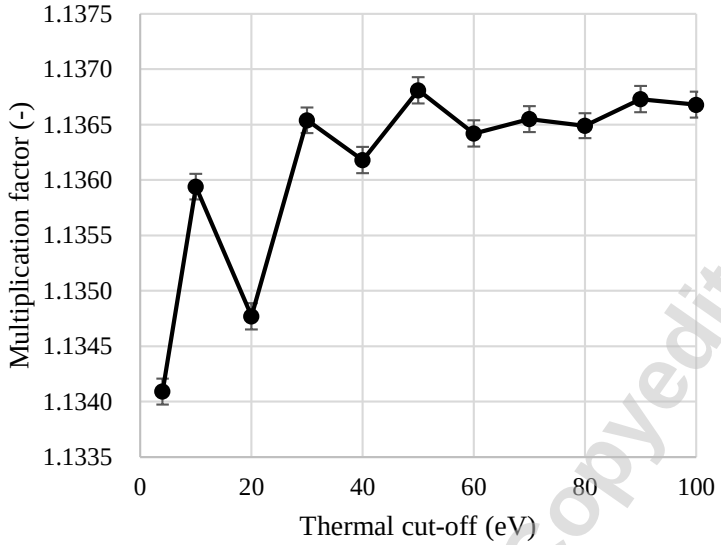

Fig. 2 Multiplication factors with varying thermal cut-off energy at BOL when fuel temperature is 1900K and moderator temperature is 300K

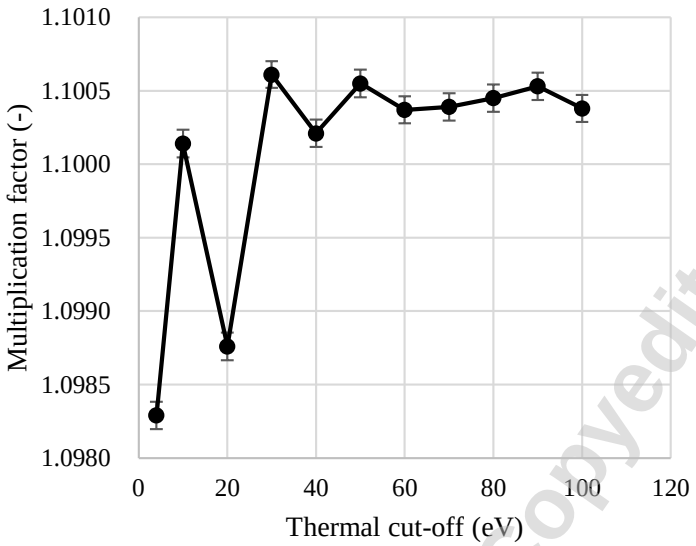

Fig. 3 Multiplication factors with varying thermal cut-off energy at EOL when fuel temperature is 1900K and moderator temperature is 300K

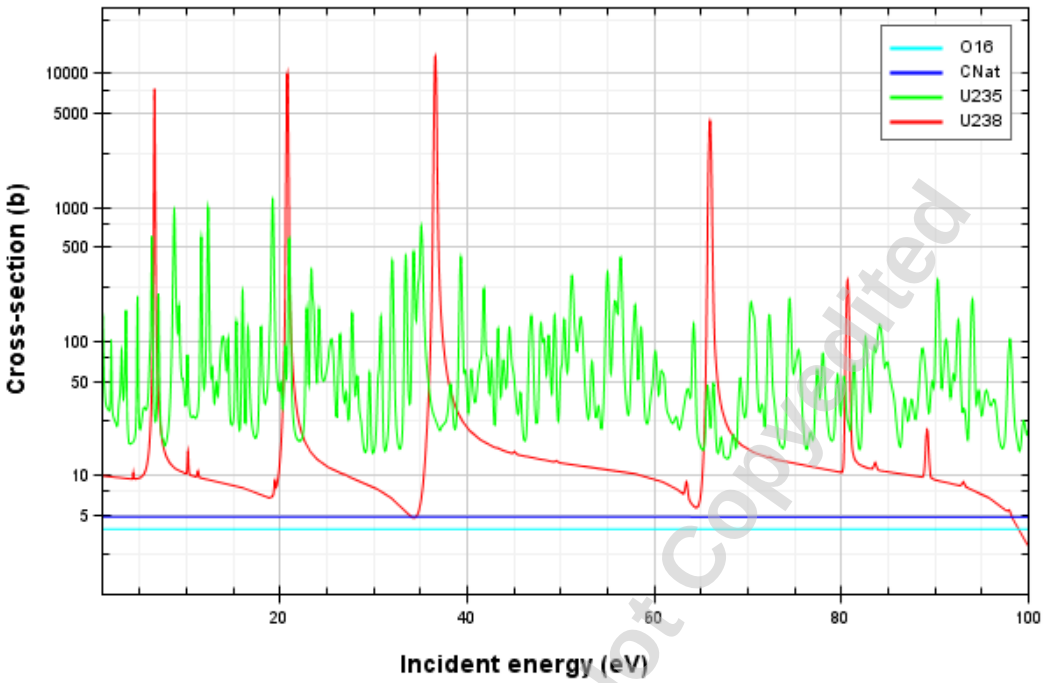

Fig. 4 Total cross-sections of carbon, O-16, U-235, and U-238

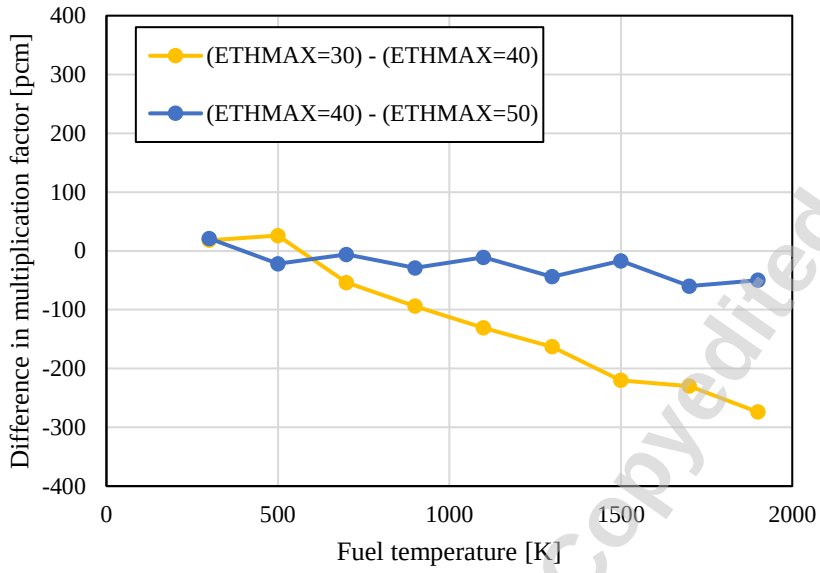

Fig. 5 Change in multiplication factor with varying ETHMAX using the exact mode at BOL

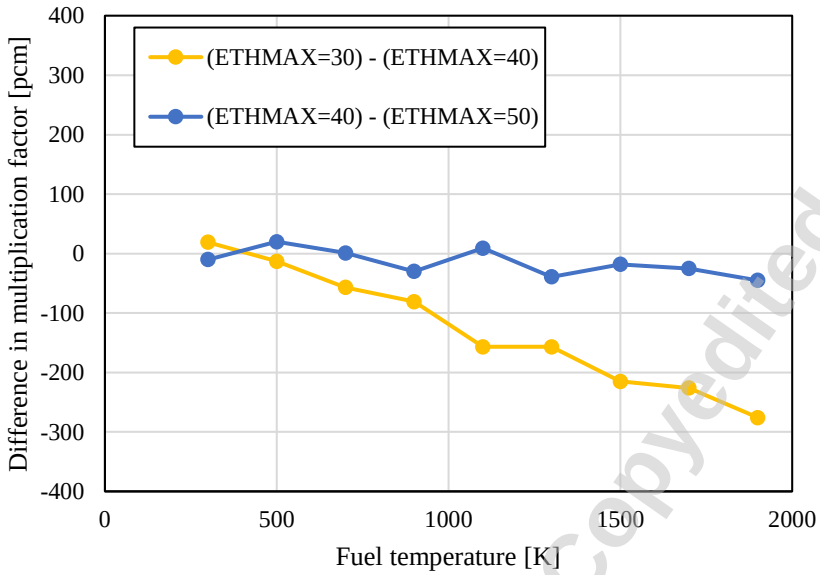

Fig. 6 Change in multiplication factor with varying ETHMAX using the exact mode at EOL

322 **Table Caption List**
323

Table 1 HTTR conditions.

Table 2 Comparison of multiplication factors with varying fuel temperatures at BOL when moderator temperature is 300K.

Table 3 Comparison of multiplication factors with varying fuel temperatures at EOL when moderator temperature is 300K.

Table 4 Comparison of multiplication factors with varying moderator temperatures at BOL when fuel temperature is 300K.

Table 5 Comparison of multiplication factors with varying moderator temperatures at EOL when fuel temperature is 300K.

Table 6 Difference in multiplication factor with varying ETHMAX using exact model at BOL when fuel temperature is 1900K.

324

325 Table 1 HTTR conditions.

ITEMS	VALUES
Core power [MWth]	30
Effective fuel length [m]	2.9
Fuel element pitch [cm]	36
Fuel compact cell pitch [cm]	5.1
Uranium enrichment [wt%]	6.7
Number of fuel element [-]	30
Linear power density [MW/cm]	3.4×10^{-3}
Core cycle [day]	660

326
327

328 Table 2 Comparison of multiplication factors with varying fuel temperatures at BOL

329 when moderator temperature is 300K.

Fuel temp. [K]	Multiplication factor with different ETHMAX [-]				Diff. [pcm]		
	[I] 4 eV	[II] 10 eV	[III] 20 eV	[IV] 30 eV	[I] -[IV]	[II] -[IV]	[III] -[IV]
400	1.23874	1.23835	1.23819	1.23866	8	-31	-47
500	1.22928	1.22895	1.22864	1.22929	-1	-34	-65
600	1.22009	1.22013	1.21955	1.22033	-24	-20	-78
700	1.21180	1.21176	1.21136	1.21214	-34	-38	-78
800	1.20357	1.20388	1.20333	1.20441	-84	-53	-108
900	1.19617	1.19645	1.19595	1.19680	-63	-35	-85
1000	1.18842	1.18922	1.18848	1.18967	-125	-45	-119
1100	1.18163	1.18231	1.18164	1.18252	-89	-21	-88
1200	1.17495	1.17578	1.17487	1.17631	-136	-53	-144
1300	1.16827	1.16941	1.16875	1.17011	-184	-70	-136
1400	1.16224	1.16350	1.16252	1.16388	-164	-38	-136
1500	1.15612	1.15746	1.15639	1.15830	-218	-84	-191
1600	1.15050	1.15186	1.15073	1.15254	-204	-68	-181
1700	1.14490	1.14639	1.14517	1.14689	-199	-50	-172
1800	1.13962	1.14131	1.13975	1.14196	-234	-65	-221
1900	1.13409	1.13594	1.13477	1.13654	-245	-60	-177

330
331

Table 3 Comparison of multiplication factors with varying fuel temperatures at EOL when moderator temperature is 300K.

Fuel temp. [K]	Multiplication factor with different ETHMAX [-]				Diff. [pcm]		
	[I] 4 eV	[II] 10 eV	[III] 20 eV	[IV] 30 eV	[I] -[IV]	[II] -[IV]	[III] -[IV]
400	1.18487	1.18418	1.18420	1.18452	35	-34	-32
500	1.17626	1.17618	1.17574	1.17618	8	0	-44
600	1.16842	1.16822	1.16803	1.16845	-3	-23	-42
700	1.16117	1.16143	1.16084	1.16166	-49	-23	-82
800	1.15455	1.15486	1.15437	1.15509	-54	-23	-72
900	1.14825	1.14848	1.14806	1.14901	-76	-53	-95
1000	1.14233	1.14284	1.14207	1.14316	-83	-32	-109
1100	1.13666	1.13718	1.13647	1.13784	-118	-66	-137
1200	1.13133	1.13203	1.13120	1.13240	-107	-37	-120
1300	1.12623	1.12687	1.12612	1.12729	-106	-42	-117
1400	1.12100	1.12195	1.12102	1.12256	-156	-61	-154
1500	1.11634	1.11736	1.11626	1.11788	-154	-52	-162
1600	1.11177	1.11276	1.11172	1.11334	-157	-58	-162
1700	1.10699	1.10851	1.10724	1.10910	-211	-59	-186
1800	1.10255	1.10408	1.10299	1.10477	-222	-69	-178
1900	1.09829	1.10014	1.09876	1.10061	-232	-47	-185

335 Table 4 Comparison of multiplication factors with varying moderator temperatures at

336 BOL when fuel temperature is 300K.

Moderator temp. [K]	Multiplication factor with different ETHMAX [-]				Diff. [pcm]		
	[I] 4 eV	[II] 10 eV	[III] 20 eV	[IV] 30 eV	[I] -[IV]	[II] -[IV]	[III] -[IV]
400	1.24583	1.24516	1.24498	1.24554	29	-38	-56
500	1.24257	1.24201	1.24176	1.24186	71	15	-10
600	1.23939	1.23846	1.23833	1.23870	69	-24	-37
700	1.23606	1.23533	1.23506	1.23525	81	8	-19
800	1.23304	1.23219	1.23190	1.23179	125	40	11
900	1.23007	1.22902	1.22886	1.22918	89	-16	-32
1000	1.22720	1.22602	1.22572	1.22593	127	9	-21
1100	1.22471	1.22345	1.22313	1.22351	120	-6	-38
1200	1.22215	1.22072	1.22019	1.22067	148	5	-48
1300	1.21968	1.21828	1.21795	1.21796	172	32	-1

337

338 Table 5 Comparison of multiplication factors with varying moderator temperatures at

339 EOL when fuel temperature is 300K.

Moderator temp. [K]	Multiplication factor with different ETHMAX [-]				Diff. [pcm]		
	[I] 4 eV	[II] 10 eV	[III] 20 eV	[IV] 30 eV	[I] -[IV]	[II] -[IV]	[III] -[IV]
400	1.19385	1.19329	1.19321	1.19334	51	-5	-13
500	1.19411	1.19330	1.19335	1.19348	63	-18	-13
600	1.19474	1.19396	1.19355	1.19391	83	5	-36
700	1.19535	1.19425	1.19410	1.19450	85	-25	-40
800	1.19599	1.19496	1.19462	1.19503	96	-7	-41
900	1.19628	1.19511	1.19476	1.19503	125	8	-27
1000	1.19678	1.19524	1.19500	1.19532	146	-8	-32
1100	1.19681	1.19542	1.19495	1.19522	159	20	-27
1200	1.19643	1.19473	1.19465	1.19474	169	-1	-9
1300	1.19584	1.19387	1.19368	1.19413	171	-26	-45

340

341 Table 6 Difference in multiplication factor with varying ETHMAX using exact model at

342 BOL when fuel temperature is 1900K.

ETHMAX Difference	Multiplication Factor Change [pcm]
(ETHMAX=30) - (ETHMAX=40)	-237
(ETHMAX=40) - (ETHMAX=50)	-24
(ETHMAX=50) - (ETHMAX=60)	-7
(ETHMAX=60) - (ETHMAX=70)	-38
(ETHMAX=70) - (ETHMAX=80)	31
(ETHMAX=80) - (ETHMAX=90)	-24
(ETHMAX=90) - (ETHMAX=100)	-2

343